A&A 494, 1137–1166 (2009)
DOI: 10.1051/0004-6361:200810371

Astronomy & Astrophysics

The Quintuplet cluster

I. A *K*-band spectral catalog of stellar sources⋆,⋆⋆,⋆⋆⋆

A. Liermann, W.-R. Hamann, and L. M. Oskinova

University of Potsdam, Institute for Physics and Astronomy, 14476 Potsdam, Germany
e-mail: adriane@astro.physik.uni-potsdam.de

Received 11 June 2008 / Accepted 10 September 2008

ABSTRACT

Context. Three very massive clusters are known to reside in the Galactic center region, the Arches cluster, the Quintuplet cluster, and the central parsec cluster, each of them rich in young hot stars. With new infrared instruments, this region is no longer obscured for the observer.
Aims. For understanding these very massive clusters, it is essential to know their stellar inventory. We provide comprehensive spectroscopic data for the stellar population of the Quintuplet cluster that will form the basis of subsequent spectral analyses.
Methods. Spectroscopic observations of the Quintuplet cluster were obtained with the Integral Field Spectrograph SINFONI-SPIFFI at the ESO-VLT. The inner part of the Quintuplet cluster was covered by 22 slightly overlapping fields, each of them of $8'' \times 8''$ in size. The spectral range comprises the near-IR *K*-band from 1.94 to 2.45 μm. The 3D data cubes of the individual fields were flux-calibrated and combined to one contiguous cube, from which the spectra of all detectable point sources were extracted.
Results. We present a catalog of 160 stellar sources in the inner part of the Quintuplet cluster. The flux-calibrated *K*-band spectra of 98 early-type stars and 62 late-type stars are provided as Online Material. Based on these spectra, we assign spectral types to all detected sources and derive synthetic K_S-band magnitudes. Our sample is complete to about the 13th *K*-magnitude. We report the detection of two hitherto unknown Wolf-Rayet stars of late WC type (WC9 or later). Radial velocities are measured and employed to assess the cluster membership. The quantitative analysis of the early-type spectra will be the subject of a subsequent paper.

Key words. catalogs – Galaxy: center – Galaxy: open cluster and associations: individual: quintuplet – infrared: stars – stars: late-type – stars: early-type

1. Introduction

The Galactic center has long been hidden from optical observation due to high extinction in the visual. Today the advanced instruments for infrared radiation give access to this region. Three surprisingly young and massive stellar clusters were found within a projected distance of 35 pc from the central black hole: the Arches, the Quintuplet, and the central cluster. These clusters are found to be rich in massive stars (Arches: Blum et al. 2001, Figer 2004, Martins et al. 2008; Quintuplet: Figer et al. 1997, 1999a, Figer 2004; Galactic center cluster: Eckart et al. 2004; Figer 2004). The prominent constellation of five infrared-bright stars gave the reason to name one of the clusters the "Quintuplet cluster" (Okuda et al. 1987, 1989). It has a projected distance of 30 pc to the Galactic center, a cluster radius of about 1 pc, and an estimated age of about 4 million years (Okuda et al. 1990; Figer et al. 1999a).

First spectroscopic observations of the five "Quintuplet proper" stars (later named Q1, Q2, Q3, Q4, and Q9 by Figer et al. 1999a) showed only a continuum without any features. Some of them have also been detected as far-IR and radio sources (Lang et al. 1997, 1999, 2005). Tuthill et al. (2006) resolved two of the original Quintuplet stars (Q2 and Q3) in space and time as colliding wind binaries, ejecting dust in the shape of a rotating "pinwheel". According to further spectroscopic studies (Figer et al. 1999a; Figer 2004), the cluster contains at least 100 O stars and 16 Wolf-Rayet stars. Two massive, evolved stars in their luminous blue variable (LBV) phase, the "Pistol star" and a second LBV candidate, have been found in the Quintuplet cluster (Geballe et al. 2000). At least two luminous stars of late spectral type K and M were found in the cluster as well.

The present paper (hereafter the "LHO catalog") provides a comprehensive spectral atlas of *K*-band spectra from stellar sources in the Quintuplet cluster. These spectra can form the basis of subsequent analysis of the luminous stellar population, which is a prerequisite for understanding the formation and evolution of this very massive cluster in its special galactic environment.

The paper is structured as follows. Section 2 gives details on the observations and data reduction. Section 3 contains the catalog with position, spectral classification, synthetic *K* mag, and radial velocity. The final Sect. 4 summarizes the catalog. The spectral atlas comprising 160 stars is shown in Table 2.

2. Observations

2.1. The data

We obtained service mode observations with the ESO VLT UT4 (Yepun) telescope between May and July 2006 using the integral field spectrograph SPIFFI of the SINFONI module that

⋆ Based on observations collected at the ESO VLT (program 077.D-0281(A)).
⋆⋆ Table 2 is also available in electronic form at the CDS via anonymous ftp to cdsarc.u-strasbg.fr (130.79.128.5) or via http://cdsweb.u-strasbg.fr/cgi-bin/qcat?J/A+A/494/1137
⋆⋆⋆ Catalog in ascii mode will be available at the CDS in July 2009.

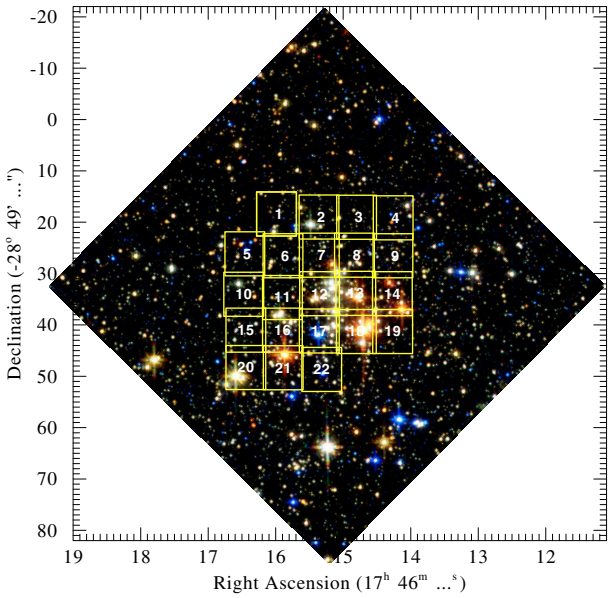

Fig. 1. The 22 observed fields, overlayed on an HST composite image (HST Heritage archive).

is equipped with a Rockwell Hawaii 2RD 2k × 2k detector (Eisenhauer et al. 2003; Bonnet et al. 2004). The adaptive optics facility could not be used since no suitable guide star is available in this field and the laser guide star was not offered during this period.

The observations consist of 22 observation blocks (OBs) covering the dense center of the Quintuplet cluster with slightly overlapping fields of view of 8″ × 8″ (see Fig. 1). The ABBA cycles were performed with an exposure time of 2 × 5 mn on each science field. The grating for the K-band (1.95–2.45 μm) provides a spectral resolution of $R \approx 4000$. Table 1 gives an overview of the observations with their date and the center coordinates of the FoV. In the same mode, standard stars were observed at similar airmass for the flux calibration of the spectra.

2.2. Data reduction

The first steps of the data reduction were performed using the SPRED software (Abuter et al. 2006). Raw frames are corrected for bad pixels, distortion, and flatfield, followed by the wavelength calibration. The slitlets are stacked into a data cube, which then consists of layers of monochromatic images. This reduction process was applied to the science exposures as well as to the standard star observations.

Sky subtraction was not performed at this stage of the data reduction, since the sky frames turned out to be contaminated by stellar sources that would create "negative stars" in the reduced data; therefore, sky frames could not be applied. The sharp emission peaks in the extracted spectra, especially those of the fainter objects, are caused by telluric OH contamination (see Fig. 2).

Further data reduction was performed with a self-written IDL cascade consisting of three parts. First, the standard star data cubes were sky-subtracted, using the monochromatic median of a pre-defined "star free" subarray of the field for each wavelength layer. Then, the standard star spectra were extracted by adding all pixels within a predefined extraction radius, mimicking a synthetic aperture. Each standard star spectrum was identified with a Kurucz model (Kurucz 1993), selected according to the spectral type (between B and G) and scaled to the 2MASS K_S-band magnitude (Skrutskie et al. 2006). The calibration curve that will be applied later to the science observations, was obtained as the ratio between the model flux and the extracted standard-star spectrum. As the Kurucz models do not reproduce the Brγ line profile perfectly, the residual feature in the calibration curve was smoothed out by interpolation between 2.15 and 2.17 μm.

Sky subtraction for the science observations was also performed with a monochromatic median of a pre-defined "star-free" subarray of each cube. Subsequently, each science observation was flux-calibrated by multiplying the cube wavelength plane with the corresponding value of the calibration curve. Then, all OBs were combined to one mosaic. The nominal telescope pointing turned out to be too imprecise for this purpose. Instead, we generated 2D images for each OB by "collapsing" the data cube to a passband image. These images were then used to determine the mutual spatial offsets between the fields by manually overlaying them on the HST composite image by Figer (HST program 7364, STScI-PRC1990-30b). Applying these offsets, all 22 OB cubes were combined into one grand mosaic cube, averaging the flux for pixels in overlapping regions.

The final part of the IDL cascade takes this grand mosaic cube and collapses it to a passband image. Then an automated search for detecting point sources was run on this 2D image. The radius to extract point sources was generally set to 4 pixels. A smaller synthetic aperture was chosen for stars that have close neighbors or are at the borders of the grand mosaic cube. In any case the applied calibration curve was based on standard star spectra extracted with the same aperture. Figure 3 shows the passband image of the grand mosaic cube overlayed with the detected sources and their running number in this "LHO" catalog.

Table 1. List of observation blocks (OBs).

OB	Name of OB	Date 2006	RA 17^h46^m	Dec $-28°49'$
229 060	Quintuplet–01	18–05	15.s99	18.″4
229 062	Quintuplet–02	01–06	15.s36	19.″0
229 064	Quintuplet–03	01–06	14.s80	19.″0
229 066	Quintuplet–04	07–06	14.s26	19.″1
229 068	Quintuplet–05	07–06	16.s46	26.″1
229 070	Quintuplet–06	07–06	15.s89	26.″5
229 072	Quintuplet–07	24–06	15.s35	26.″4
229 074	Quintuplet–08	24–06	14.s83	26.″4
229 076	Quintuplet–09	24–06	14.s26	26.″5
229 078	Quintuplet–10	24–06	16.s47	34.″0
229 080	Quintuplet–11	24–06	15.s90	34.″7
229 082	Quintuplet–12	24–06	15.s37	33.″9
229 084	Quintuplet–13	24–06	14.s81	33.″9
229 086	Quintuplet–14	24–06	14.s27	33.″9
229 088	Quintuplet–15	24–06	16.s44	41.″0
229 090	Quintuplet–16	24–06	15.s90	41.″0
229 092	Quintuplet–17	29–06	15.s35	41.″2
229 094	Quintuplet–18	29–06	14.s81	41.″3
229 096	Quintuplet–19	29–06	14.s27	41.″3
229 098	Quintuplet–20	30–06	16.s44	48.″3
229 100	Quintuplet–21	01–07	15.s89	48.″3
229 102	Quintuplet–22	01–07	15.s32	48.″7

3. The catalog

3.1. Coordinates and identification

To derive the coordinates, we superimpose the map of the detected sources (Fig. 3) on the HST image of the field (Fig. 1). The

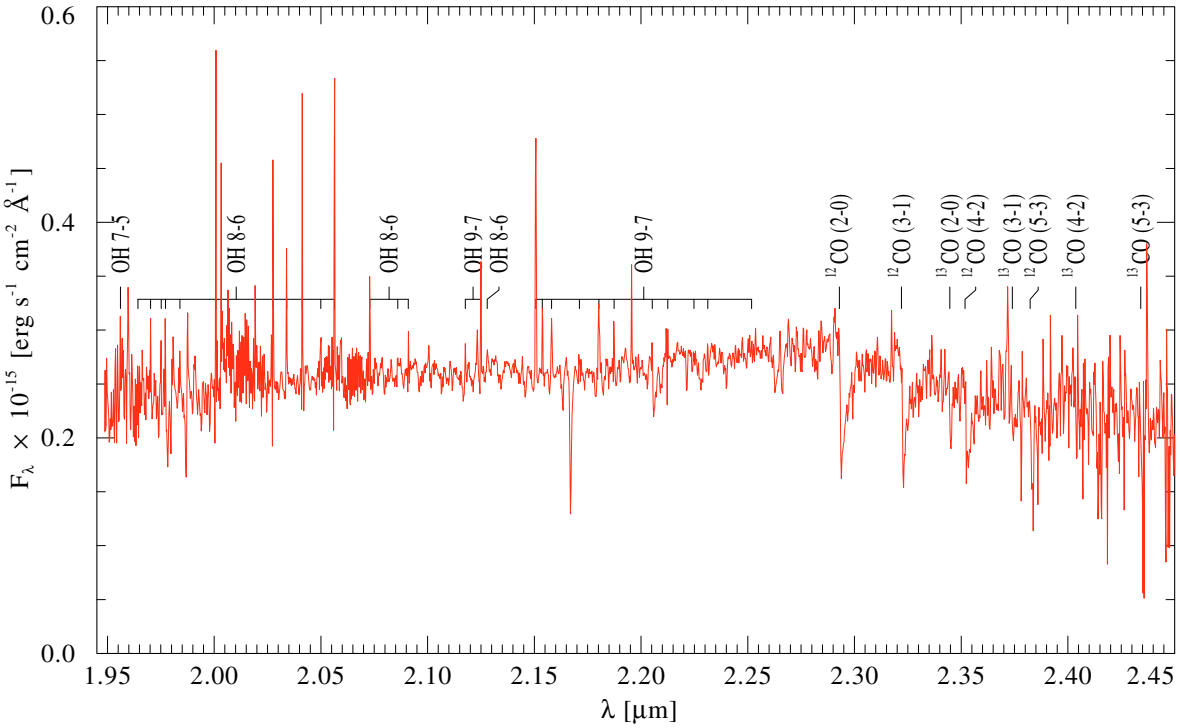

Fig. 2. Flux-calibrated *K*-band spectrum of an M star (LHO 4). Identifications for the telluric OH lines are from Rousselot et al. (2000). The prominent molecular absorption bands are produced by CO. Their identifications are based on Gorlova et al. (2006) and Wallace & Hinkle (1997). Note the discrimination between the isotopes ^{12}CO and ^{13}CO.

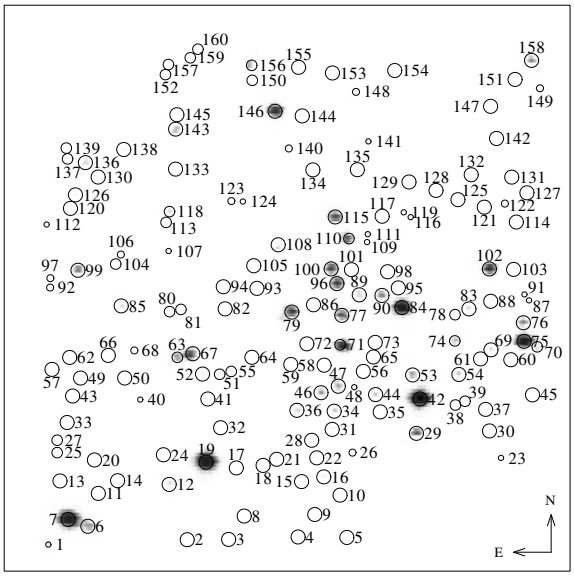

Fig. 3. Image of the collapsed grand mosaic cube. Open circles mark the detected sources with their running number in this "LHO" catalog. Circle radii correspond to the extraction radius for the object spectra.

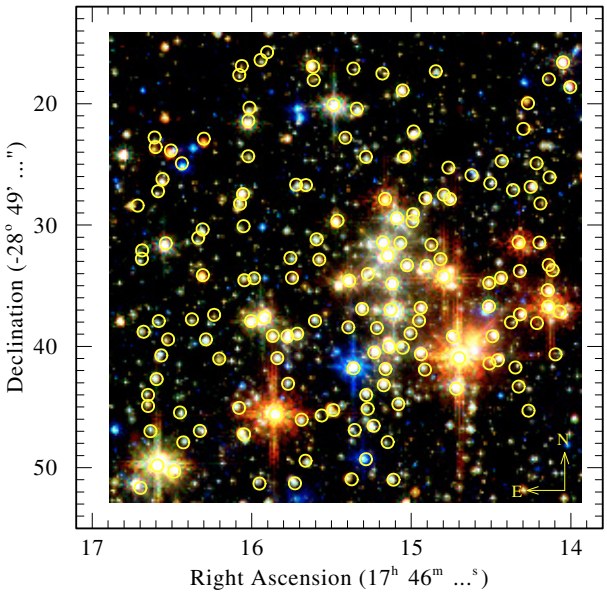

Fig. 4. Detected sources in the Quintuplet cluster as overlay on a detail of the HST composite image (compare Fig. 3 for object identification; figures not to scale).

well-determined positions of foreground stars from the USNO-B catalog (Monet et al. 2003) are used to construct the mapping between the pixel positions and the celestial coordinates. An overlay image with coordinates is shown in Fig. 4.

Table 2 lists all 160 extracted sources. Column 1 gives the running number in this "LHO" catalog, followed by the coordinates in Cols. 2 and 3. The SIMBAD database was employed to find possible cross-identifications (see Col. 7).

Lang et al. (2005) report that for their radio sources QR 1, QR 2, and QR 3 no counterparts are found in the near-IR. This led these authors to discuss the possibility that the sources are ultracompact H II regions with ongoing star formation. We confirm the absence of *K*-band counterparts for these radio sources in our data.

3.2. Spectral classification

Classification of OB stars was performed according to Hanson et al. (1996, 2005) and Morris et al. (1996), concentrating on the

Table 2. Catalog of stars detected in the central Quintuplet cluster field.

LHO No.	RA 17^h46^m [s]	Dec –28°49′ [″]	K_S [mag]	Spectral type	RV [km s^{-1}]	Alias names & remarks
1	16.70	51.4	10.9	O3–8 I fe	117	[FMG99] 8 em. line star
2	15.95	51.3	13.2	O7.5–B2 I-II e	117	
3	15.73	51.3	12.5	O6–8 I f	117	
4	15.37	51.0	13.0	M1 II	104	
5	15.11	51.0	12.6	O6.5–9 I f?	104	
6	16.49	50.3	9.9	M7 I	124	
7	16.59	49.8	7.6	M6 I	124	**Q 7**, qF 192, NSV 23780, MGM 5-7
8	15.66	49.4	12.8	K2 I	-16f	
9	15.28	49.3	13.6	O4–6 I f?	99	
10	15.15	47.9	14.0	O7–9 I f	109	
11	16.42	47.9	13.4	O3–7 I–II e	114	
12	16.05	47.2	11.3	M1 I	44f	[GMC99] D 3605
13	16.64	47.0	13.5	O6–B2 I	84:	
14	16.33	47.0	13.3	K3 II	144	
15	15.35	46.9	13.8	O4–7 I f	104	
16	15.24	46.5	11.9	O8.5–9.7 I ab? f?	104	qF 197?
17	15.69	46.0	12.2	O3–7 I-II f?	94	
18	15.56	45.7	13.6	O7–8 I f	104	
19	15.85	45.6	7.2	WC8/9d +OB	104	**Q 3**, GCS 4, MGM 5-3, WR 102ha, qF 211, [LY2004] QX 3, [GSL2002] 66, [NHS93] 26 “pinwheel” star
20	16.45	45.5	13.5	K5 II	160	
21	15.49	45.3	11.9	K4 I	94	
22	15.27	45.1	12.8	K2 I	119	
23	14.27	45.3	13.6	O3–6 I–II f	85	
24	16.08	45.1	12.4	O7–9 I f? e	95	
25	16.65	44.9	13.1	M0 II	120	
26	15.08	44.8	13.3	O5–B0 I f?	95	
27	16.65	44.0	13.9	K1 II	-35:f	
28	15.28	44.0	12.3	O7–9 I e	110	
29	14.72	43.5	9.9	O9–B2 I f? e	120	
30	14.33	43.3	13.6	K5 II	155:	
31	15.17	43.2	12.1	O9–B1 I f?	85	
32	15.77	43.1	13.3	B1.5–3 I f?	47:f	
33	16.60	42.7	12.8	O9–B3 I-II f	87	
34	15.16	41.9	11.3	WC8	95:	WR 102g, qF 235S
35	14.91	41.9	12.8	O9–B2 I e?	105	
36	15.36	41.8	11.3	K0? I	90	USNO-B1.000611-0602187? (Monet et al. 2003)
37	14.35	41.7	14.1	O9–B3 I-II	105:	
38	14.51	41.4	12.9	K2 II	105	
39	14.46	41.1	12.2	O7–B1 I f?	85:	[GMC99] D 3606
40	16.20	41.0	13.5	M1 II	37f	
41	15.84	41.0	12.5	O9–B1 I f	107	
42	14.70	41.0	6.7	WC9d + OB	115	**Q 2**, WR 102dc, GCS 3-2, MGM 5-1, qF 231, [LFG99] QR 7, [LY2004] QX 5, [NHS93] 24, “pinwheel” star
43	16.57	40.8	13.1	K0 I	132	
44	14.94	40.6	11.1	O7–9 I f?	110	
45	14.10	40.7	14.0	O7–B1 I	105	
46	15.23	40.5	10.7	O7–B1 I f?	95	MGM 5-11b?
47	15.14	40.0	10.4	WC8	115	**Q 11**, MGM 5-11a, [NWS90] G, WR 102f, qF 235N, [FMG99] 2, possible binary (van der Hucht 2006)
48	15.05	40.1	12.0	O7.5–9.5 I f?	110	
49	16.52	39.4	13.4	K0? I	157	
50	16.29	39.4	12.7	O7–B1 I f	97	[LY2004] QX 4?
51	15.78	39.2	11.4	O7–9 I f	97	
52	15.87	39.1	11.9	M0 I	147	[GMC99] D 334
53	14.74	39.2	10.5	M3 I	125	
54	14.49	39.2	11.6	O7–9 I-II f?	80:	
55	15.72	38.9	12.0	O7–9 I f	87	
56	15.00	38.9	12.6	O7–9 I f?	120	
57	16.68	38.8	13.3	K1 I	127	
58	15.22	38.5	12.9	O9–B1 I-II p?	96:	
59	15.39	38.5	13.3	O9–B1 I	96:	
60	14.21	38.1	13.0	O9–B1 I f?	96:	
61	14.38	38.0	13.6	O7–9 I f?	96:	
62	16.58	37.9	14.0	O7–B1 I–II f	107	
63	16.00	37.9	10.3	M2 I	122	

Table 2. continued.

LHO No.	RA 17^h46^m [s]	Dec $-28°49'$ [″]	K_S [mag]	Spectral type	RV [km s^{-1}]	Alias names & remarks
64	15.60	37.9	12.9	O7–9 I f?	106:	
65	14.95	37.9	12.8	O3–7 I eq?	106:	
66	16.38	37.8	13.6	K3 II	127	
67	15.92	37.6	9.6	WN9	112	**Q 8**, WR 102hb, MGM 5-8, qF 240
68	16.24	37.4	14.1	K2 II	147	
69	14.32	37.4	11.5	O6–9.7 I f?	96:	
70	14.07	37.1	11.0	O7–8 I f	91	
71	15.13	37.0	8.8	WN9	116	**Q 10**, MGM 5-10, qF 241, WR 102ea, [NWS90] F, [LFG99] QR 5
72	15.31	36.9	11.9	O4–6 I eq?	76	
73	14.94	36.8	11.7	O6.5–7 I f?	111:	
74	14.51	36.7	10.9	O9.5–B1 I ab? f	96	[LY2004] QX 1, qF 242?, [GMC99] D 309
75	14.14	36.7	7.9	WC9?d	116:	**Q 1**, WR 102da, qF 243, GCS 3-4, MGM 5-1, narrow and weak lines
76	14.15	35.4	10.3	WC9d	137:	NEW!!!
77	15.12	34.8	9.6	O6–8 I f eq	97	**Q 12**, MGM 5-12, qF 278, [NWS90] E
78	14.51	34.8	11.9	M1 I	142	qF 252?
79	15.39	34.6	9.3	WC9d	132	**Q 6**, qF 250, MGM 5-6, [NWS90] B, re-classified
80	16.05	34.6	12.9	K4 I–II	147	
81	15.99	34.4	13.2	O3–4 II/III? f	87:	
82	15.75	34.3	12.9	K5 II	117	
83	14.44	34.4	11.4	M2 I	117	qF 252?
84	14.80	34.2	7.8	WC9d	127:	**Q 4**, MGM 5-4, WR 102dd, GCS 3-1, qF 251
85	16.31	34.1	11.4	M3 I	127	
86	15.27	34.0	12.2	K0? I	137:	
87	14.11	33.7	13.4	K4 II	52f	
88	14.32	33.8	13.3	O3–4 III f	107:	
89	15.03	33.3	11.1	O7.5–8.5 I f	97	[LY2004] QX 2?
90	14.91	33.4	10.3	O7–9.5 I f e?	87	GCS 3I H II region?, [GSL2002] 63?
91	14.14	33.3	13.5	K5 II	67	
92	16.69	32.8	13.9	O8–9.7 I	87	
93	15.58	32.8	12.5	K3 I	–33f	
94	15.76	32.7	13.3	O7–B1 I f?	87	
95	14.82	32.8	11.9	K1 I	77	GCS 3I H II region?, [GSL2002] 63?
96	15.15	32.5	9.3	O6–8 I f e	132	MGM 5-13b?
97	16.69	32.1	14.1	O7–B2 I-II	97:	
98	14.87	31.6	12.7	K4 I	77	
99	16.54	31.5	10.1	WN9	127	WR 102i, qF 256, [GMC99] D 215
100	15.18	31.4	9.4	O6–8 I f e	67	**Q 13**, MGM 5-13a, [NWS90] D, [LFG99] QR 6, qF 257
101	15.07	31.5	11.9	O6–8 I f?e?	87	
102	14.33	31.4	9.2	WC9?d	97	**Q 9**, MGM 5-9, WR 102db, qF 258, GCS 3–3, narrow and weak lines
103	14.20	31.4	12.7	O7–9 I f	97:	
104	16.34	31.1	13.6	O9–B2 I-II f?	97	
105	15.60	31.2	12.6	O7–9 I f?	107	
106	16.31	30.4	12.7	O7–9.5 I	112	
107	16.05	30.1	13.9	O7–9 I f?	106:	
108	15.46	29.6	10.7	M3 I	127	qF 269, [GMC99] D 322, [NWS90] A
109	14.99	29.7	13.0	O7–9 I f?	97:	
110	15.09	29.4	10.6	O6–8 I f (Of/WN?)	117	**Q 15**, qF 270S, MGM 5-15, [LFG99] QR 4, [NWS90] C
111	14.99	29.1	12.4	O8–9 I f?	107:	
112	16.72	28.4	12.8	K4 I–II	6f	
113	16.07	28.2	12.5	K2 I	136	
114	14.19	28.2	13.9	K4 II	137	
115	15.16	27.8	8.6	M2 I	137	**Q 5**, qF 270N, V 4646 Sgr, MGM 5-5
116	14.76	27.9	12.2	M1 I–II	57f	
117	14.91	27.8	12.1	K0? I	142:	
118	16.05	27.4	11.5	O6–9 I f?	56f	
119	14.80	27.5	12.7	K0? I	17:f	
120	16.59	27.2	13.9	O5–9 I–II f?	106:	
121	14.36	27.1	13.4	K1 I	97	
122	14.25	26.9	11.6	O7–9.7 I e	107	
123	15.72	26.7	12.8	K1 I	36f	
124	15.66	26.8	13.5	K0? I	32:f	
125	14.50	26.6	13.5	O7–9 I-II	97:	
126	16.56	26.2	12.5	O7–9 I f?	106:	
127	14.13	26.1	13.5	K1 II	97:	
128	14.62	25.9	13.5	O3–5 I	97:	
129	14.77	25.3	13.4	K3 II	137	
130	16.44	24.9	13.9	O7.5–9 I-II e?	96:	

Table 2. continued.

LHO No.	RA 17^h46^m [s]	Dec $-28°49'$ [″]	K_S [mag]	Spectral type	RV [km s^{-1}]	Alias names & remarks
131	14.22	24.9	13.5	K2 II	17f	
132	14.43	24.7	13.0	O7–9 I–II f?	97	
133	16.02	24.3	13.4	K3 II	156:	
134	15.28	24.4	13.5	O9–B2 I f?	97:	
135	15.05	24.4	11.7	K4 I	–33f	
136	16.51	23.9	11.2	M2 I	76	
137	16.60	23.6	13.1	K2 I	176	
138	16.30	22.9	11.9	M1 I	146	
139	16.61	22.8	13.5	O7–9 I f?	101:	
140	15.41	22.8	14.2	K3 II	133:	
141	14.99	22.3	11.5	O9.7–B1 I	103:	
142	14.30	22.1	13.5	K3 II	122	
143	16.02	21.4	10.5	O7–B0 I	115:	qF 301, [GMC99] D 271
144	15.34	20.4	11.8	O7–9 I	124:	
145	16.01	20.3	12.7	O7–9 I	115:	
146	15.49	20.1	8.7	O6–8 I f?	124	**Q 14**, qF 307A, MGM 5-14
147	14.27	19.96	12.8	M0 II	126	
148	15.05	18.9	11.3	O7–9 I	109	
149	14.00	18.6	12.1	O7–9.7 I	101	
150	15.61	18.1	13.4	K1 I	169:	
151	14.14	17.99	14.0	K0? II	56f	
152	16.08	17.6	14.0	O6.5-8 I-II f	95	
153	15.18	17.5	13.5	K4 II	59f	
154	14.85	17.3	12.5	O7–9 I	109:	
155	15.36	17.1	13.9	K2 II	69:	
156	15.61	16.9	10.4	M0 I	169	[GMC99] D 307
157	16.06	16.9	14.5	O3–4 II/III?	115	
158	14.05	16.6	10.5	WN9	106	WR 102d, qF 320, [LGF99] QR 8, [GMC99] D278?
159	15.94	16.4	13.9	O7–9 I	105	
160	15.90	15.8	14.6	K1 II	165	

List of catalogs (SIMBAD identifier and reference): GCS – Kobayashi et al. (1983) $Q \rightarrow GMM$ catalog – Glass et al. (1990) [NWS90] – Nagata et al. (1990) MGM – Moneti et al. (1992, 1994) [NHS93] – Nagata et al. (1993) qF – Figer et al. (1999a) [FMG99] – Figer et al. (1999b) [GMC99] – Glass et al. (1999) [LFG99] – Lang et al. (1999, 2003, 2005) [GSL2002] – Giveon et al. (2002) [LY2004] – Law & Yusef-Zadeh (2004) WR – van der Hucht (2006) *Spectral classification*: OB stars – Hanson et al. (1996, 2005) and Morris et al. (1996): using H I 2.1661 μm Br γ, He I 2.0587 μm, 2.1127/37 μm, 2.1499 μm, 2.1623 μm, He II 2.1891 μm, C IV triplet around 2.0796 μm, N III/C III 2.1155 μm WR stars – Crowther et al. (2006): applying line ratio C IV (2.079)/C III (2.108) for WC and He II (2.189)/Br γ (2.166) for WN stars KM giant stars – Wallace & Hinkle (1997), Kleinmann & Hall (1986), Goorvitch (1994): ^{12}CO and ^{13}CO bands, subclasses following González-Fernández et al. (2008), see text Sect. 3.2.
Magnitudes: Synthetic K_S magnitudes from our calibrated spectra, see Sect. 3.3 for details.
Radial velocity and Cluster membership: *RV* measured with the position of the Br γ line for early-type stars and CO (2–0) band head for late-type stars. Uncertain measurements are marked with ":", foreground objects are indicated by "f", see Sect. 3.4.

most prominent lines in the K-band region (H I 2.1661 μm Brγ, He I 2.0587 μm, He II 2.1891 μm, C IV triplet around 2.0796 μm, N III/C III 2.1155 μm) for comparison with their template spectra. Additional He I lines (2.1127/37 μm, 2.1499 μm, 2.1623 μm) were employed to distinguish supergiants from giants. Spectral peculiarities are given in Table 2 in the classical nomenclature and are followed by "?" in uncertain cases, such as noisy spectra or blends with atmospheric OH lines. An example of an O star spectrum is shown in Fig. 5.

Wolf-Rayet stars have been classified following the criteria from Crowther et al. (2006). For WC stars we measured line equivalent widths and determined the ratio C IV 2.079 μm/C III 2.108 μm. The ratio He II (2.189 μm)/Brγ (2.166 μm) was used for the subtype classification of WN stars. A strongly increasing continuum with wavelength was considered to indicate the dominance of warm dust emission, marked with "d" in the spectral classification.

Our sample contains eleven previously known WR stars, four WN, and seven WC. Two new WR stars are found in our sample, LHO 76 and 79.

We could not identify LHO 76 with any previously known source. Therefore we claim that this object is a newly discovered WR star in the Quintuplet cluster, and its spectral type is WC9d (Fig. 6). Following the naming scheme of van der Hucht (2001), this star would squeeze in between the known stars WR 102da and WR 102db. A possible scheme to rename this group could be LHO 76 → WR 102db (new), WR 102db (old) → WR 102dc (new), WR 102dc (old) → WR 102dd (new), WR 102dd (old) → WR 102de (new).

The other new WR star – LHO 79 – has already been listed by Figer et al. (1999a) as qF 250, but classified as <B0 I. We re-classify this star as spectral type WC9d (see Fig. 7). This increases the total number of WR stars in the sample to 13.

All WC stars turned out to be of late subtype, WC8 and WC9. In all cases the WC9 spectra display dust emission, while the two WC8 spectra (LHO 34 and 47) are free of such contamination.

The stellar spectra of LHO 75 and 102 are particularly drowned in dust emission. The diluted stellar lines appear unusually narrow. The identification of the classification line C III 2.110 μm is questionable, making the WC9 subtype uncertain ("WC9?d") for these two stars.

Late-type stars were classified using the dominating features of the absorption bands caused by the CO first overtone. We find

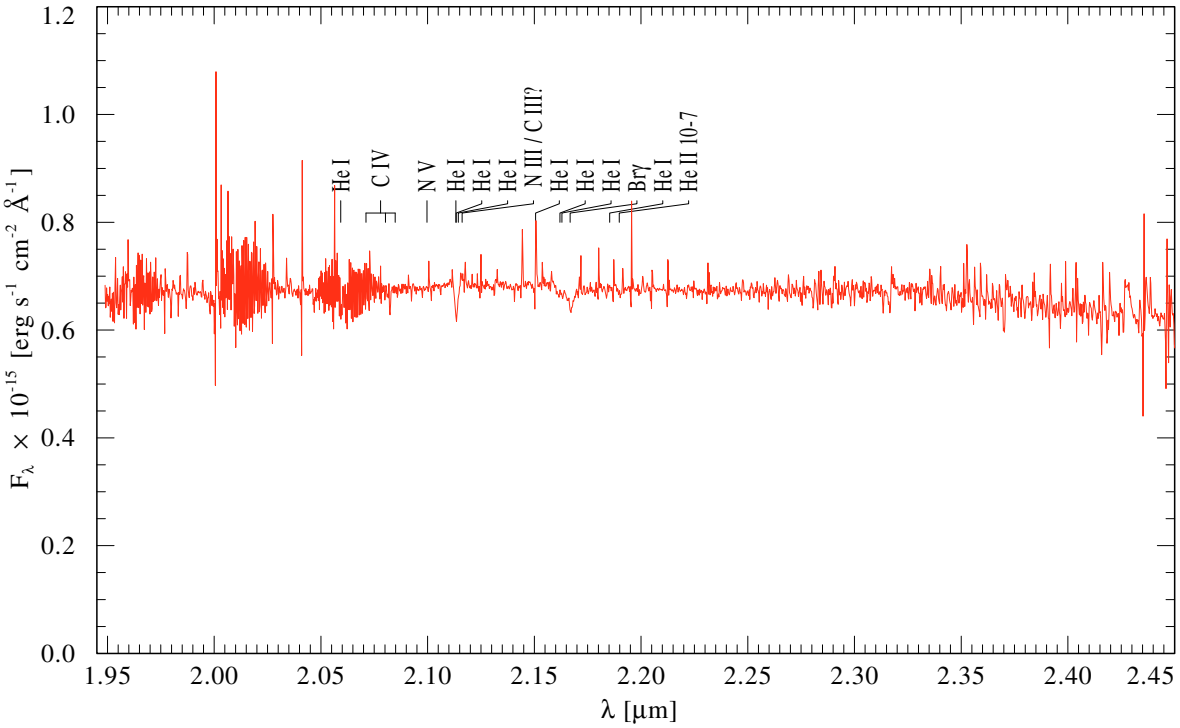

Fig. 5. Flux-calibrated *K*-band spectrum of an O star (LHO 55) with line identifications as used for spectral classification.

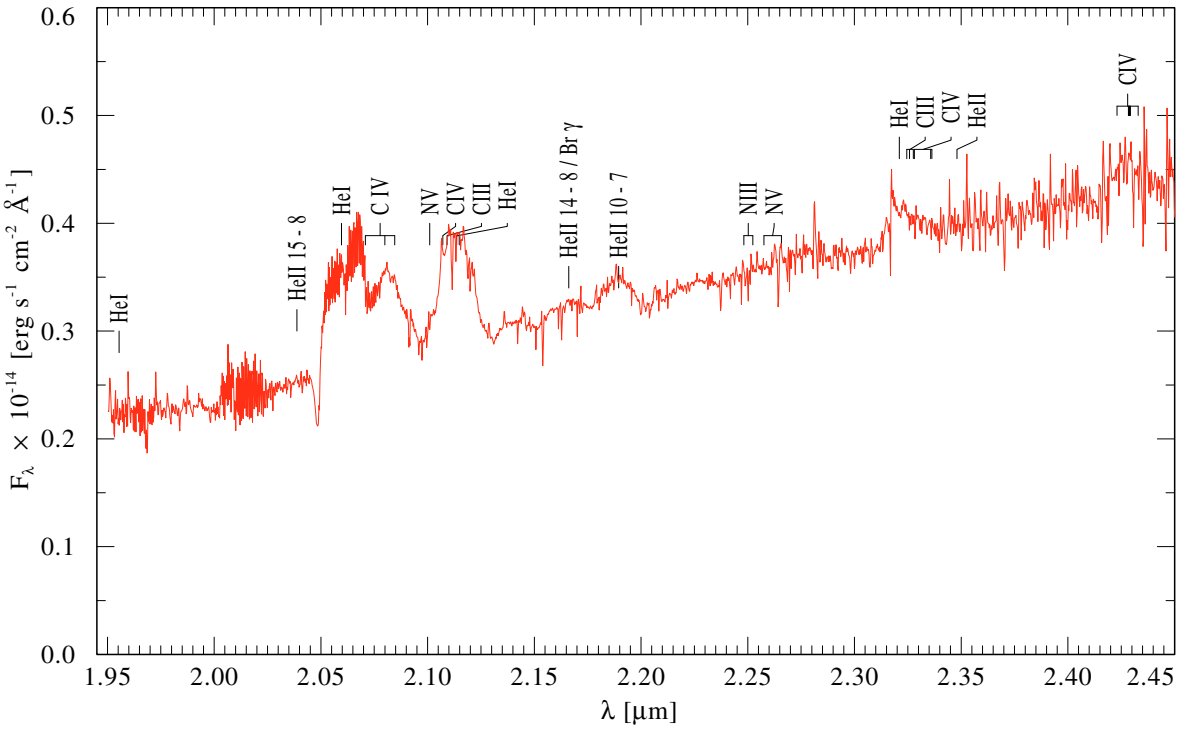

Fig. 6. Flux-calibrated *K*-band spectrum of the newly detected WR star LHO 76 with line identifications. The spectral type is WC9d.

both ^{12}CO and ^{13}CO absorption, the latter indicating late type (super-)giant stars (Goorvitch 1994; Wallace & Hinkle 1997; Kleinmann & Hall 1986). Figure 2 shows LHO 4 as an example of an M star. We then measured the equivalent width of the band-head CO (2–0) to determine the effective temperature

$$T_{\rm eff} = 4895 - 62 \times {\rm EW(CO)} \quad (1)$$

and spectral subtypes of the stars

$$G = 0.56 \times {\rm EW(CO)} - 3.0, \quad (2)$$

following González-Fernández et al. (2008). The integer number G ranges from 0 to 13 representing the subtypes from K0 to M7, e.g. $G = 6$ gives M0. Derived G values were rounded to the next integer to determine the subtypes as listed in Table 2. Both relations are only applicable for (super-) giant stars, an assumption that is justified by the presence of the ^{13}CO band absorption mentioned above, as well as by the synthetic $K_{\rm S}$ magnitudes, see Sect. 3.3. For seven stars, the measured equivalent width was so small that the resulting G value was slightly in the negative

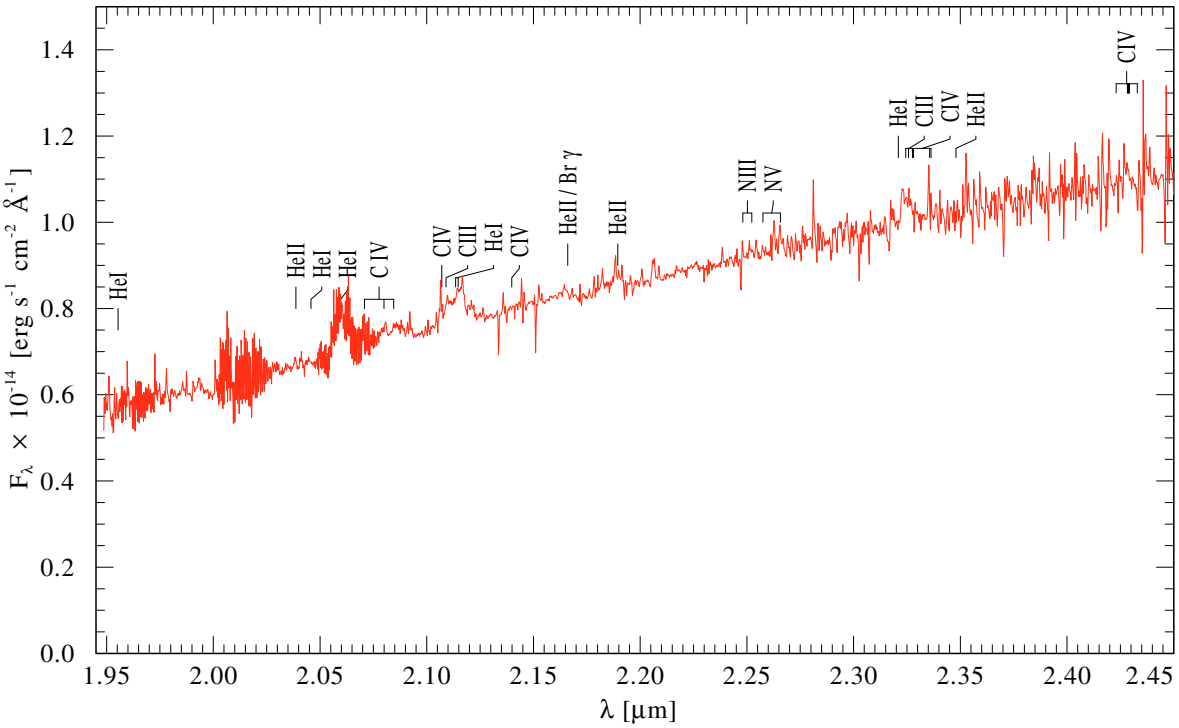

Fig. 7. Flux-calibrated K-band spectrum of Q 6 (LHO 79) showing broad emission line features superimposed on a warm-dust continuum. The spectral class is WC9d, revising the classification by Figer et al. (1999a) who gave "<B0 I" for the alias-named object qF 250.

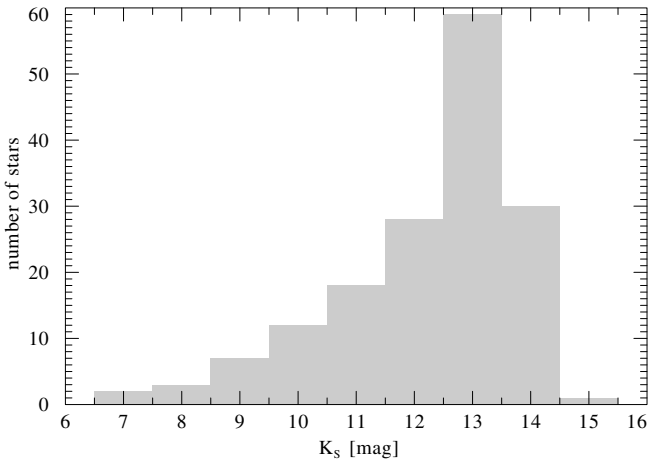

Fig. 8. Histogram of the synthetic K-band magnitudes with a bin size of 1 mag, indicating a photometric completeness of the catalog up to K_S = 13 mag.

range. We classify these stars as "K0?" in Table 2 to indicate that they might be of an earlier spectral subtype.

3.3. Photometry

From our flux-calibrated spectra, we derived synthetic K-band magnitudes. For comparability we chose the K_S (K "short") filter of 2MASS, which is centered at 2.159 μm, and used the calibration constant from Cohen et al. (2003) for the photometric zero point. Fifteen LHO stars are in common with the sample of Glass et al. (1999). We compare our derived magnitudes with their values and obtain a mean agreement within 0.4 mag. The magnitudes obtained for all catalog objects are listed in Table 2. The number of stars per magnitude is shown in Fig. 8 as a histogram. The distribution follows a power law up to

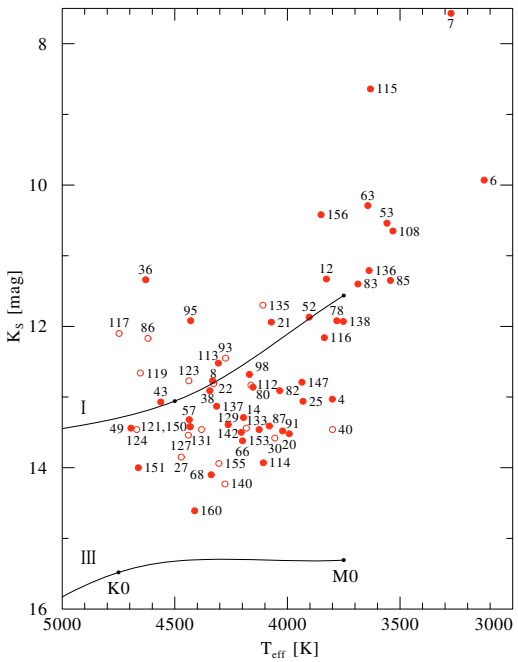

Fig. 9. K magnitude vs. T_{eff} for the late-type stars of our sample, identified by their LHO number (Table 2). Open circles denote stars for which the radial velocity is uncertain or definitely indicates that they are foreground objects. The solid line interpolates between corresponding values from Kurucz models for G0, K0, and M0 stars. The upper line refers to supergiant models (luminosity class I) and the lower line to giants (luminosity class III).

K_S = 13 mag, which indicates that our catalog is complete to this magnitude.

To determine the approximate luminosity class of our late-type stars, we plotted their K_S magnitudes versus their determined effective temperature (Fig. 9). For comparison we take

Table 3. Spectral-type distribution.

Spectral type	No. of stars
WN	4
WC	9
WR total	*13*
O	60
B	25
OB total	*85*
K	43
M	19
KM total	*62*
Total	160

models (Kurucz 1993) of G0, K0, and M0 stars of the luminosity classes I and III, with assumed masses of 1.1 $M_\odot$, 0.8 $M_\odot$, and 0.4 $M_\odot$, respectively. The model fluxes are scaled for the adopted cluster distance of 8 kpc (Reid 1993) and diminished according to the average extinction of $A_K = 3.28$ mag (Figer et al. 1999a). The models are connected in Fig. 9 by solid lines to mark the approximate regions of the corresponding luminosity class. Most of our sample stars scatter around the line for supergiants. Some stars are slightly less bright and therefore are assigned to luminosity class II. A few stars, LHO 6, LHO 7, and LHO 115, seem to be extremely bright, see Fig. 9.

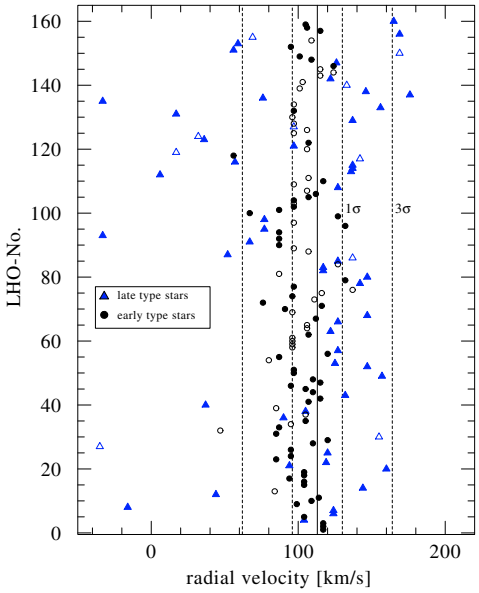

Fig. 10. Radial velocities of the catalog stars. Circles denote early-type stars, triangles late-type stars. Open symbols are for uncertain values due to noisy spectra. The solid vertical line indicates $\overline{RV}_{\rm QPM} = 113$ km s^{-1}, while the dashed lines indicate intervals of $\pm\sigma$ and $\pm 3\sigma$ (± 17 km s^{-1} and ± 51 km s^{-1}), respectively.

3.4. Cluster membership

For all spectra in the catalog, we measured the wavelength of a prominent feature, Br γ for early-type stars and CO (2–0) for late-type stars, and derived the radial velocity for the individual objects (Fig. 10 and Table 2). Heliocentric corrections were applied to the radial velocities. The measurement errors can be expected to be maximal ± 37 km s^{-1} from the nominal spectral resolution of the instrument. The results may be more uncertain for some of the more noisy spectra (marked with ":" in Table 2).

Assuming that the fifteen bright Quintuplet stars from the QPM list (Glass et al. 1990) are real cluster members, we derived their mean radial velocity $\overline{RV}_{\rm QPM} = 113$, with a standard deviation of $\sigma = 17$ km s^{-1}. This is in good agreement with the 130 km s^{-1} found by Figer et al. (1999a). For a prediction of the internal velocity dispersion of the cluster, we followed Kroupa (2002). Despite the reported young age, we assumed a virialized cluster, a star formation efficiency between 20 and 40 % (Kroupa 2002), and a stellar mass in the range of $10^{3.8-4.2}$ $M_\odot$ (Figer et al. 1999a). This yields a radial velocity dispersion of 8–18 km s^{-1}, which agrees with the determined standard deviation of the fifteen QPM stars, $\sigma = 17$ km s^{-1}. Therefore we consider the 3σ interval around $\overline{RV}_{\rm QPM}$ as a criterion for cluster membership. As Fig. 10 shows, there are a few stars in our sample with lower radial velocities, primarily of late spectral type. They have to be considered as foreground objects, i.e. K or M dwarfs, and are marked "f" in Table 2.

4. Summary

We present the first K-band spectral catalog of 160 stellar sources in the central region of the Quintuplet cluster. Integral field spectra were obtained with the SINFONI-SPIFFI on UT4 from May to July 2006. Our catalog comprises flux-calibrated spectra of 98 early-type stars (OB and WR) and 62 late-type stars (K to M) with a spectral resolution of $R \approx 4000$. Table 3 lists the number of stars per spectral class.

All 160 sources are listed in Table 2 with their LHO number, which was assigned to the source in our data reduction and identification processes (Col. 1), the determined coordinates of the source (Cols. 2 and 3), and the derived synthetic $K_{\rm S}$ magnitude (Col. 4). The spectral type is given in Col. 5. radial velocities (RV) are given in Col. 6, together with an assessment whether this RV value indicates a foreground object ("f"). Finally we give a complete list of aliases and cross-identification with previous catalogs and surveys in Col. 7. Note that about 100 objects of our list are cataloged here for the first time.

Two new WR stars of WC spectral subtype are found in our sample, LHO 76 and 79, increasing the number ratio WC:WN in the Quintuplet cluster to 10:6 in total (9:4 contained in our field). WC stars are outstandingly frequent and bright in the Quintuplet cluster. For comparison, the WC:WN number ratios from van der Hucht (2006) are 0:17 for the Arches cluster, 12:17 for the central cluster, and 8:19 for Westerlund I, respectively. A difference to the solar neighbourhood WC:WN ratio of 38:25 (van der Hucht 2001) can be seen. A detailed analysis of the WR star subsample with the Potsdam models for expanding atmospheres (PoWR) is in preparation.

Among the new stars in our catalog there are a number of late-type supergiants. In case the red supergiants (RSG) are real cluster members, as supported by their radial velocities, the question of age and coeval evolution of the Quintuplet cluster has to be addressed again in this context.

The spectral atlas of the catalog is shown in Fig. 11; 98 stars are of early spectral type (O, B and WR), and 62 of late type (K and M). A few spectra are dominated by dust emission. For each detected source it comprises the flux-calibrated K-band spectrum in the wavelength range from 1.95 to 2.45 μm. The spectra are binned to 4 Å , some spectra suffer from atmospheric OH emission lines. The "LHO" numbering of the stars refers to Table 2. The wavelength scale refers to the local standard of rest.

Acknowledgements. We thank the anonymous referee for helpful suggestions on the manuscript. Furthermore, the authors thank A. Barniske for the valuable help in preparing the Phase 2 material. T. Szeifert and D. Nürnberger supported A. L. with very useful discussions on the ESO SINFONI-SPIFFI instrument, data reduction pipelines, its results and technical details in handling the huge amount of data. Furthermore A.L. thanks H. Todt for supporting, discussing, and writing IDL routines on integral field spectroscopy data in the reduction process. This publication makes use of data products from the Two Micron All Sky Survey, which is a joint project of the University of Massachusetts and the Infrared Processing and Analysis Center/California Institute of Technology, funded by the National Aeronautics and Space Administration and the National Science Foundation. This research has made use of the SIMBAD database, operated at CDS, Strasbourg, France. A. Liermann is supported by the Deutsche Forschungsgemeinschaft (DFG) under grant HA 1455/19.

References

Abuter, R., Schreiber, J., Eisenhauer, F., et al. 2006, New Astron. Rev., 50, 398
Blum, R. D., Schaerer, D., Pasquali, A., et al. 2001, AJ, 122, 1875
Bonnet, H., Abuter, R., Baker, A., et al. 2004, The Messenger, 117, 17
Cohen, M., Wheaton, W. A., & Megeath, S. T. 2003, AJ, 126, 1090
Crowther, P. A., Hadfield, L. J., Clark, J. S., Negueruela, I., & Vacca, W. D. 2006, MNRAS, 372, 1407
Eckart, A., Moultaka, J., Viehmann, T., Straubmeier, C., & Mouawad, N. 2004, ApJ, 602, 760
Eisenhauer, F., Abuter, R., Bickert, K., et al. 2003, in Instrument Design and Performance for Optical/Infrared Ground-based Telescopes, ed. M. Iye, & A. F. M. Moorwood, Proc. SPIE, 4841, 1548
Figer, D. F. 2004, in The Formation and Evolution of Massive Young Star Clusters, ed. H. J. G. L. M. Lamers, L. J. Smith, & A. Nota, ASP Conf. Ser., 322, 49
Figer, D. F., McLean, I. S., & Najarro, F. 1997, ApJ, 486, 420
Figer, D. F., McLean, I. S., & Morris, M. 1999a, ApJ, 514, 202
Figer, D. F., Morris, M., Geballe, T. R., et al. 1999b, ApJ, 525, 759
Geballe, T. R., Najarro, F., & Figer, D. F. 2000, ApJ, 530, L97
Giveon, U., Sternberg, A., Lutz, D., Feuchtgruber, H., & Pauldrach, A. W. A. 2002, ApJ, 566, 880
Glass, I. S., Moneti, A., & Moorwood, A. F. M. 1990, MNRAS, 242, 55P
Glass, I. S., Matsumoto, S., Carter, B. S., & Sekiguchi, K. 1999, MNRAS, 304, L10
González-Fernández, C., Cabrera-Lavers, A., Hammersley, P. L., & Garzón, F. 2008, A&A, 479, 131
Goorvitch, D. 1994, ApJS, 95, 535
Gorlova, N., Lobel, A., Burgasser, A. J., et al. 2006, ApJ, 651, 1130
Hanson, M. M., Conti, P. S., & Rieke, M. J. 1996, ApJS, 107, 281
Hanson, M. M., Kudritzki, R.-P., Kenworthy, M. A., Puls, J., & Tokunaga, A. T. 2005, ApJS, 161, 154
Kleinmann, S. G., & Hall, D. N. B. 1986, ApJS, 62, 501
Kobayashi, Y., Okuda, H., Sato, S., Jugaku, J., & Dyck, H. M. 1983, PASJ, 35, 101
Kroupa, P. 2002, MNRAS, 330, 707
Kurucz, R. L. 1993, VizieR Online Data Catalog, 6039, 0
Lang, C. C., Goss, W. M., & Wood, D. O. S. 1997, ApJ, 474, 275
Lang, C. C., Figer, D. F., Goss, W. M., & Morris, M. 1999, AJ, 118, 2327
Lang, C. C., Johnson, K. E., Goss, W. M., & Rodríguez, L. F. 2005, AJ, 130, 2185
Law, C., & Yusef-Zadeh, F. 2004, ApJ, 611, 858
Martins, F., Hillier, D. J., Paumard, T., et al. 2008, A&A, 478, 219
Monet, D. G., Levine, S. E., Canzian, B., et al. 2003, AJ, 125, 984
Moneti, A., Glass, I., & Moorwood, A. 1992, MNRAS, 258, 705
Moneti, A., Glass, I. S., & Moorwood, A. F. M. 1994, MNRAS, 268, 194
Morris, P. W., Eenens, P. R. J., Hanson, M. M., Conti, P. S., & Blum, R. D. 1996, ApJ, 470, 597
Nagata, T., Woodward, C. E., Shure, M., Pipher, J. L., & Okuda, H. 1990, ApJ, 351, 83
Nagata, T., Hyland, A. R., Straw, S. M., Sato, S., & Kawara, K. 1993, ApJ, 406, 501
Okuda, H., Shibai, H., Kobayashi, Y., et al. 1987, in Star Forming Regions, ed. M. Peimbert & J. Jugaku, IAU Symp., 115, 556
Okuda, H., Shibai, H., Nakagawa, T., et al. 1989, in The Center of the Galaxy, ed. M. Morris, IAU Symp., 136, 281
Okuda, H., Shibai, H., Nakagawa, T., et al. 1990, ApJ, 351, 89
Reid, M. J. 1993, ARA&A, 31, 345
Rousselot, P., Lidman, C., Cuby, J.-G., Moreels, G., & Monnet, G. 2000, A&A, 354, 1134
Skrutskie, M. F., Cutri, R. M., Stiening, R., et al. 2006, AJ, 131, 1163
Tuthill, P., Monnier, J., Tanner, A., et al. 2006, Science, 313, 935
van der Hucht, K. A. 2001, VizieR Online Data Catalog, 3215, 0
van der Hucht, K. A. 2006, A&A, 458, 453
Wallace, L., & Hinkle, K. 1997, ApJS, 111, 445